

Effects of point defects on the phase diagram of vortex states in high- T_c superconductors in $\vec{B} \parallel c$ axis

Yoshihiko Nonomura* and Xiao Hu

National Research Institute for Metals, Tsukuba, Ibaraki 305-0047, Japan
(November 17, 2000)

The phase diagram for the vortex states of high- T_c superconductors with point defects in $\vec{B} \parallel c$ axis is drawn by large-scale Monte Carlo simulations. The vortex slush (VS) phase is found between the vortex glass (VG) and the vortex liquid (VL) phases. The first-order transition between this novel normal phase and the VL phase is characterized by a sharp jump of the density of dislocations. The first-order transition between the Bragg glass (BG) and the VG or VS phases is also studied. These two transitions are compared with the melting transition between the BG and the VL phases.

74.60.Ge, 74.62.Dh, 74.25.Dw

Vortex states in high- T_c superconductors in $\vec{B} \parallel c$ axis have been intensively studied. The melting transition in pure systems has now been understood very well. On the other hand, phase diagrams observed experimentally are more complicated than that of pure systems. Effects of impurities turn out to be essential in real materials. In the present Letter, point defects are taken into account as the simplest impurity.

A schematic phase diagram of vortex states in high- T_c superconductors with point defects is given in the inset of Fig. 1. The three phases in this figure have been observed in $\text{YBa}_2\text{Cu}_3\text{O}_{7-\delta}$ (YBCO) and $\text{Bi}_2\text{Sr}_2\text{CaCu}_2\text{O}_{8+y}$ (BSCCO). The flux-line lattice phase in pure systems is replaced by two kinds of glass phases. In the weak-field region, the Bragg glass (BG) phase [1] is stable. This phase is characterized by the power-law decay of correlation functions of vortex positions [2,1] and the triangular Bragg pattern of the structure factor. In the strong-field region, the vortex glass (VG) phase is expected to exist. This phase is first proposed by Fisher *et al.* [3] on the basis of the phase ordering. Although recent numerical studies including the screening effect [4,5] suggest the absence of this phase ordering, the VG can also be defined on the basis of the positional ordering. The positional VG is a counterpart of the BG, and more stable than the phase-coherent VG. [6]

The BG–VG phase boundary was studied analytically, [7–9] essentially based on the Lindemann criterion. Numerically, difference between the BG and the VG phases was discussed, [10,11] and the overall phase diagram was obtained recently. [12,13] However, studies based on thermodynamic quantities are still lacking.

Quite recently, Nishizaki *et al.* has found a sharp jump of the resistivity [14,15] and the magnetization [15] in optimally-doped YBCO in the vortex liquid (VL) region (see the inset of Fig. 1). They pointed out that this might be the transition to the vortex slush (VS) phase, which was originally introduced in irradiated YBCO. [16] Similar anomalies were also observed in BSCCO. [17–20]

In the present Letter, we compose the phase diagram on the basis of anomalies of thermodynamic quantities.

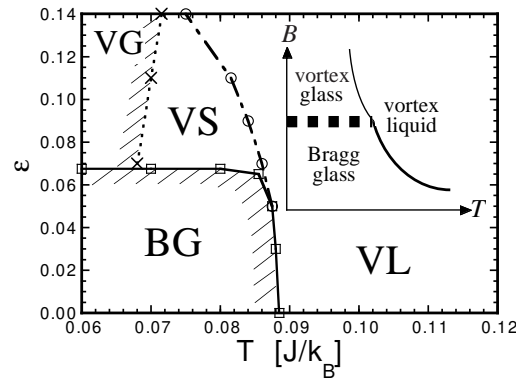


FIG. 1. e – T phase diagram of the model with $\Gamma = 20$. Shaded phases exhibit superconductivity. Schematic B – T phase diagram is shown in the inset for comparison.

Results of the present simulations are summarized as the phase diagram in the pinning-strength (e)–temperature (T) plane (Fig. 1). The first-order melting transition occurs between the BG and the VL phases as in pure systems. [21,22] A first-order transition line stretches from the melting line into the VL region dividing the VS and the VL phases. The VS–VL phase boundary is characterized by a sharp jump of the density of dislocations in the ab plane. The VG phase exists at much lower temperatures. The boundary between the BG and the VG or VS phases is almost independent of temperature, and this phase transition is of first order. The structure of this phase diagram is quite similar to the B – T phase diagram including the VS phase observed experimentally.

Our formulation is based on the three-dimensional anisotropic, frustrated XY model on a simple cubic lattice, [23,21]

$$\mathcal{H} = - \sum_{i,j \in ab \text{ plane}} J_{ij} \cos(\phi_i - \phi_j - A_{ij}) - \frac{J}{\Gamma^2} \sum_{m,n \parallel c \text{ axis}} \cos(\phi_m - \phi_n) , \quad (1)$$

$$A_{ij} = \frac{2\pi}{\Phi_0} \int_i^j \mathbf{A}^{(2)} \cdot d\mathbf{r}^{(2)}, \quad (2)$$

with the periodic boundary condition. The screening effect is not included in this model. A uniform magnetic field is applied along the c axis, and its strength is proportional to the averaged number of flux lines per plaquette, f . Point defects are introduced as the plaquettes which consist of four weaker couplings and are randomly distributed in the ab plane with probability p . Couplings are given by $J_{ij} = (1 - \epsilon)J$ ($0 < \epsilon < 1$) on the point defects, and $J_{ij} = J$ elsewhere. Here we concentrate on the model with $\Gamma = 20$, $f = 1/25$ and $p = 0.003$. The lower critical point [24,25] is not within the scope of the present study. The system size is $L_x = L_y = 50$ and $L_c = 40$, which is large enough to describe the melting transition of the pure system ($\epsilon = 0$).

For each ϵ , Monte Carlo simulations are started from a very high temperature, and systems are gradually cooled down. After such annealing, further equilibration and measurement are performed at each temperature. Typical simulation times are $4 \sim 12 \times 10^7$ Monte Carlo steps (MCS) for equilibration, and $2 \sim 4 \times 10^7$ MCS for measurement. We calculate the internal energy e , the specific heat C , the helicity modulus along the c axis Υ_c , and the phase difference between the nearest-neighbor ab planes $\langle \cos(\phi_n - \phi_{n+1}) \rangle$, together with the ratio of entangled flux lines to total flux lines $N_{\text{ent}}/N_{\text{flux}}$, [22] the density of dislocations in the ab plane ρ_d , and the structure factor of flux lines in the ab plane. The helicity modulus [23,21] is proportional to the superfluid density, and is the order parameter of superconductivity. The inter-layer phase difference is related [26] to the frequency of the Josephson plasma resonance (JPR). [27,28]

BG–VL and VS–VL phase transitions.—Temperature dependence of e , C , Υ_c and $\langle \cos(\phi_n - \phi_{n+1}) \rangle$ at $\epsilon = 0.05$, 0.07 and 0.11 is displayed in Figs. 2(a)–(d). The BG–VL transition is observed at $\epsilon = 0.05$, and the VS–VL one at $\epsilon = 0.07$ and 0.11. In both cases, jumps of e and $\langle \cos(\phi_n - \phi_{n+1}) \rangle$ and the δ -function peak of C are observed at the melting temperature T_m or the slush temperature T_{sl} . The finite latent heats $Q = \Delta e$ indicate that these phase transitions are of first order. The anomalies of the VS–VL transition at $\epsilon = 0.07$ (the starting point of this phase transition) are as large as those of the BG–VL transition at $\epsilon = 0.05$, and gradually lose sharpness as ϵ is increased (see Figs. 2(c) and 2(d)). The most important difference between these two transitions is seen in Υ_c . In the BG–VL transition, this quantity appears discontinuously at T_m . On the other hand, Υ_c remains vanishing for $T < T_{\text{sl}}$ in the VS–VL transition, and its proliferation at lower temperatures signals the phase transition to the positional VG phase. [29] In other words, the BG–VL transition is the superconducting–normal phase transition, while the VS–VL transition occurs between two normal phases. The absence of superconductivity both in the VS and the VL phases does not contradict the existence of the critical point [14–16] at which the first-order VS–VL transition line terminates.

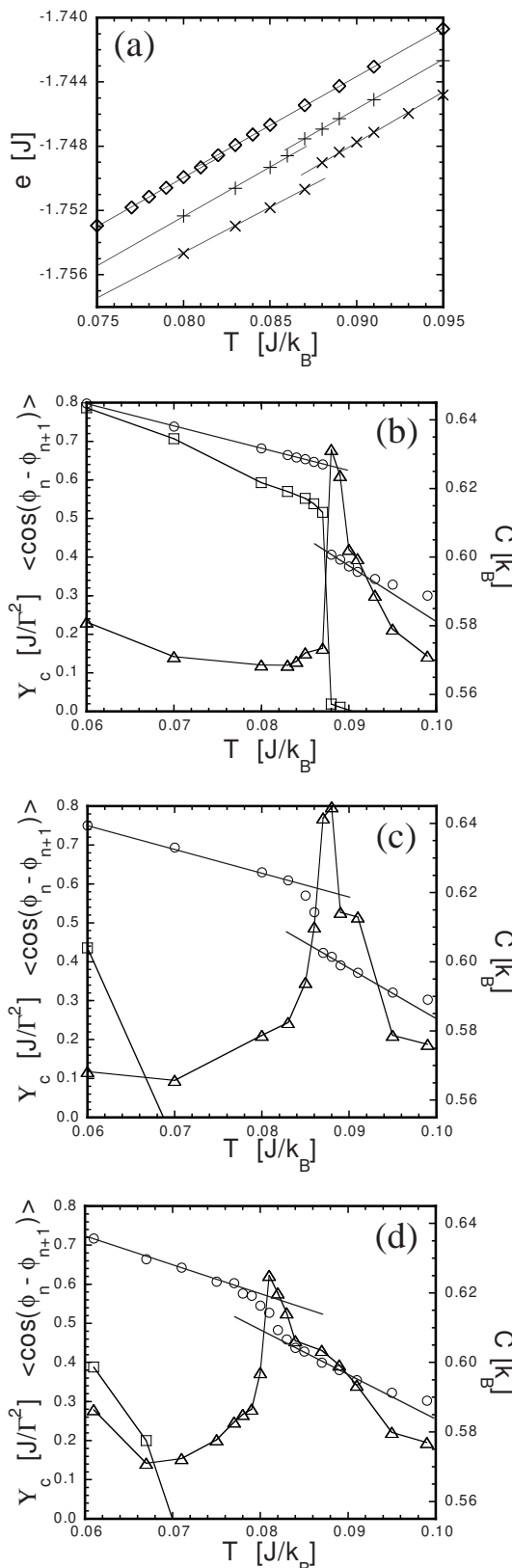


FIG. 2. Temperature dependence of (a) e at $\epsilon = 0.05$ (\times), 0.07 (+) and 0.11 (\diamond), and C (\triangle), Υ_c (\square) and $\langle \cos(\phi_n - \phi_{n+1}) \rangle$ (\circ) at (b) $\epsilon = 0.05$, (c) 0.07 and (d) 0.11. The origin of e is varied for each ϵ in (a).

Direct observation of flux lines also reveals the difference between these two first-order transitions. Temperature dependence of $N_{\text{ent}}/N_{\text{flux}}$ and ρ_d at $\epsilon = 0.05$ and $\epsilon = 0.11$ is displayed in Figs. 3(a) and 3(b), respectively. As in pure systems, [22] $N_{\text{ent}}/N_{\text{flux}}$ shows a sharp jump at T_m (Fig. 3(a)), while temperature dependence of this quantity is continuous around T_{sl} (Fig. 3(b)). The quantity ρ_d shows sharp jumps both at T_m and T_{sl} . This behavior is consistent with Kierfeld and Vinokur's theory, [30] where the free energy is expressed as a function of ρ_d , and the phase boundaries are determined by jumps of ρ_d . The structure factors on both sides of the transition temperatures are also calculated. A ring-like pattern is seen in the VL phase both at $\epsilon = 0.05$ (Fig. 3(a)) and $\epsilon = 0.11$ (Fig. 3(b)), as in pure systems. [21] In the BG–VL transition at $\epsilon = 0.05$, the clear triangular Bragg pattern for $T < T_m$ represents the formation of a hexatic quasi long-range order. In the VS–VL transition at $\epsilon = 0.11$, the obscure Bragg pattern with a 6-fold symmetry for $T < T_{\text{sl}}$ stands for islands of short-ranged hexatic structures divided by dislocations. Such interpretations of the Bragg patterns are consistent with the results for $N_{\text{ent}}/N_{\text{flux}}$ and ρ_d . That is, the drop of ρ_d occurs even when merely a short-ranged structure is formed in the ab plane, while the drop of $N_{\text{ent}}/N_{\text{flux}}$ is observed only when a lattice structure appears in the bulk system.

BG–VG and BG–VS phase transitions.—Pinning-strength dependence of e and $\langle \cos(\phi_n - \phi_{n+1}) \rangle$ is shown in Figs. 4(a) and 4(b) for $T = 0.06, 0.07$ and $0.08 J/k_B$. The finite latent heats Q indicate that these phase transitions are of first order. The quantity $\langle \cos(\phi_n - \phi_{n+1}) \rangle$ jumps simultaneously, which is consistent with Gaifullin *et al.*'s JPR experiment of BSCCO. [31] Since the anomalies are always observed between $\epsilon = 0.065$ and 0.070 , the phase boundary is almost independent of temperature as shown in Fig. 1. We also find a sudden jump of $N_{\text{ent}}/N_{\text{flux}}$ on this phase boundary, which is consistent with theoretical predictions. [7,9]

The jumps of e and $\langle \cos(\phi_n - \phi_{n+1}) \rangle$ (abbreviated as $\Delta \langle \cos \rangle$ from now on) on this almost-flat phase boundary are about one order smaller than those on the melting line. For example, $\Delta \langle \cos \rangle \approx 0.036$ at $T = 0.07 J/k_B$ on this phase boundary, while $\Delta \langle \cos \rangle \approx 0.22$ at $\epsilon = 0.05$ on the melting line. Difference between these two transitions becomes more apparent when the ratio of the jump of the Josephson energy $\Delta e_J = -(J/\Gamma^2)\Delta \langle \cos \rangle$ to Q is analyzed. On the melting line, this ratio is about one half, e.g. $\Delta e_J \approx 5.5 \times 10^{-4} J$ and $Q \approx 1.1 \times 10^{-3} J$ at $\epsilon = 0.05$, as in extremely anisotropic pure systems. [32] On the other hand, this ratio is about unity on this almost-flat phase boundary, e.g. $Q \approx \Delta e_J \approx 9.0 \times 10^{-5} J$ at $T = 0.07 J/k_B$. The latter result shows a sharp contrast to the JPR experiment of BSCCO, where $\Delta e_J/Q \gg 1$ seems to be satisfied. [33]

Discussions.—On the melting line of pure systems, $\Delta \langle \cos \rangle$ is proportional to $\Gamma^2 f$ and gradually approaches

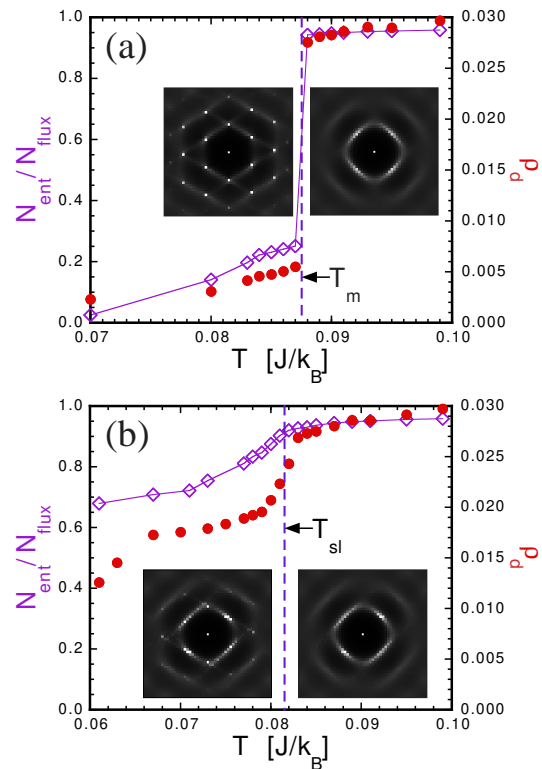


FIG. 3. Temperature dependence of $N_{\text{ent}}/N_{\text{flux}}$ (\diamond) and ρ_d (\bullet) at (a) $\epsilon = 0.05$ and (b) $\epsilon = 0.11$. Structure factors at $T = 0.087$ and $0.088 J/k_B$ are displayed in (a), and those at $T = 0.080$ and $0.083 J/k_B$ are displayed in (b).

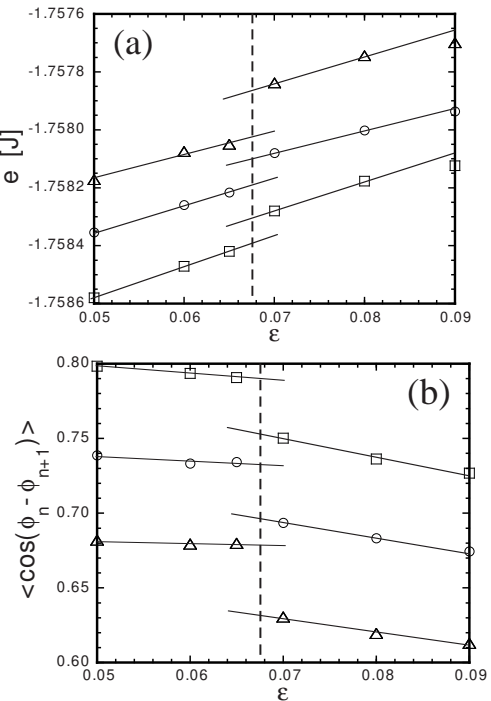


FIG. 4. Pinning-strength dependence of (a) e and (b) $\langle \cos(\phi_n - \phi_{n+1}) \rangle$ at $T = 0.06$ (\square), 0.07 (\circ) and $0.08 J/k_B$ (\triangle). The origin of e is varied for each T in (a).

a saturated value, [34] $\Delta\langle\cos\rangle \approx 0.3$. [35,31] When the anisotropy is as small as that of YBCO ($\Gamma \approx 7 \sim 8$), $\Delta\langle\cos\rangle$ is small both on the melting line and on the BG–VG phase boundary. In the present system ($\Gamma = 20$), $\Delta\langle\cos\rangle$ (≈ 0.22 at $\epsilon = 0.05$) is as large as the saturated value on the melting line, while it is small on the BG–VG/VS phase boundary. Therefore, a jump in $\langle\cos(\phi_n - \phi_{n+1})\rangle$ inevitably occurs in the VL region, which results in the VS–VL phase transition. On the other hand, when the anisotropy is as large as that of BSCCO ($\Gamma \geq 150$), $\Delta\langle\cos\rangle$ has reached the saturated value both on the melting line and on the BG–VG phase boundary as shown experimentally. [31] In such a case, it might be difficult to observe a jump of $\langle\cos(\phi_n - \phi_{n+1})\rangle$ outside of the BG phase by the JPR, [35,33] even if the VS–VL phase boundary exists in BSCCO.

Finally, the present results summarized in Fig. 1 are compared with analytic studies related to the VS phase in literature. When Worthington *et al.* [16] proposed the VS–VL transition line as a reminiscent of the melting line in pure systems, the BG phase was out of the scope. Ikeda [36] derived a phase diagram consisting of the VG, the VS and the VL phases, and argued that the BG phase and the VS phase cannot coexist. Quite recently, he modified his argument and proposed a possible phase diagram including both the BG and the VS phases. [37] However, he simply assumed the existence of the BG phase, which cannot be derived within his framework. Recently Kierfeld and Vinokur [30] obtained a phase diagram consisting of the BG phase and a first-order transition line stretching from the melting line into the VL region with a critical point. Although they interpreted this transition line as the VG–VL one, it turns out to correspond to the VS–VL one as shown in the present study. We believe that the present simulations are the first theoretical derivation of the phase diagram consisting of four phases (Fig. 1) based on anomalies of thermodynamic quantities and from a single model.

We would like to thank Y. Matsuda and T. Nishizaki for communications. One of us (Y. N.) also thanks K. Kadowaki and R. Ikeda for sending their preprints. Numerical calculations were performed on Numerical Materials Simulator (NEC SX-5) at National Research Institute for Metals, Japan.

* E-mail: nono@nrim.go.jp

- [1] T. Giamarchi and P. Le Doussal, Phys. Rev. Lett. **72**, 1530 (1994); Phys. Rev. B **52**, 1242 (1995).
- [2] T. Nattermann, Phys. Rev. Lett. **64**, 2454 (1990).
- [3] D. S. Fisher, M. P. A. Fisher, and D. A. Huse, Phys. Rev. B **43**, 130 (1991).
- [4] F. O. Pfeiffer and H. Rieger, Phys. Rev. B **60**, 6304 (1999).
- [5] H. Kawamura, J. Phys. Soc. Jpn. **69**, 29 (2000).
- [6] T. Nattermann and S. Scheidl, Advances in Physics **49**, 607 (2000).
- [7] D. Ertas and D. R. Nelson, Physica C **272**, 79 (1996).
- [8] J. Kierfeld, T. Nattermann, and T. Hwa, Phys. Rev. B **55**, 626 (1997).
- [9] T. Giamarchi and P. Le Doussal, Phys. Rev. B **55**, 6577 (1997).
- [10] M. J. P. Gingras and D. A. Huse, Phys. Rev. B **53**, 15193 (1996).
- [11] S. Ryu, A. Kapitulnik, and S. Doniach, Phys. Rev. Lett. **77**, 2300 (1996).
- [12] A. van Otterlo, R. T. Scalettar, and G. T. Zimányi, Phys. Rev. Lett. **81**, 1497 (1998).
- [13] R. Sugano, T. Onogi, K. Hirata, and M. Tachiki, Physica B **284-288**, 803 (2000).
- [14] T. Nishizaki, K. Shibata, T. Sasaki, and N. Kobayashi, Physica C (Proc. of M2S-HTSC-VI) in press.
- [15] K. Shibata *et al.*, preprint.
- [16] T. K. Worthington *et al.*, Phys. Rev. B **46**, 11 854 (1992).
- [17] D. T. Fuchs *et al.*, Phys. Rev. Lett. **80**, 4971 (1998).
- [18] T. Blasius *et al.*, Phys. Rev. Lett. **82**, 4926 (1999).
- [19] B. Khaykovich *et al.*, Phys. Rev. B **61**, R9261 (2000).
- [20] K. Kimura *et al.*, J. Low Temp. Phys. **117**, 1471 (1999), Physica B **284-288**, 717 (2000); K. Kimura, S. Kamisawa, and K. Kadowaki, Physica C (Proc. of ISS 2000) in press.
- [21] X. Hu, S. Miyashita, and M. Tachiki, Physica C **282-287**, 2057 (1997); Phys. Rev. Lett. **79**, 3498 (1997); Phys. Rev. B **58**, 3438 (1998).
- [22] Y. Nonomura, X. Hu, and M. Tachiki, Phys. Rev. B **59**, R11 657 (1999).
- [23] Y.-H. Li and S. Teitel, Phys. Rev. Lett. **66**, 3301 (1991); Phys. Rev. B **47**, 359 (1993).
- [24] M. Roulin *et al.*, Phys. Rev. Lett. **80**, 1722 (1998).
- [25] L. M. Paulius *et al.*, Phys. Rev. Lett. **61**, R11 910 (2000).
- [26] L. N. Bulaevskii, M. P. Maley, and M. Tachiki, Phys. Rev. Lett. **74**, 801 (1995).
- [27] M. Tachiki, T. Koyama, and S. Takahashi, Phys. Rev. B **50**, 7065 (1994).
- [28] Y. Matsuda *et al.*, Phys. Rev. Lett. **75**, 4512 (1995); **78**, 1972 (1997).
- [29] Since the screening effect is not included in the XY model, even the phase-coherent VG may be stable. However, glass orderings measured by Υ_c are not phase-coherent ones but positional ones. We believe that the structure of the phase diagram given in Fig. 1 will not change even when the screening effect is taken into account.
- [30] J. Kierfeld and V. Vinokur, Phys. Rev. B **61**, R14 928 (2000).
- [31] M. B. Gaifullin *et al.*, Phys. Rev. Lett. **84**, 2945 (2000).
- [32] A. E. Koshelev, Phys. Rev. B **56**, 11 201 (1997).
- [33] Y. Matsuda, private communication.
- [34] Y. Nonomura and X. Hu, Physica B **284-288**, 435 (2000); Physica C (Proc. of M2S-HTSC-VI) in press.
- [35] T. Shibauchi *et al.*, Phys. Rev. Lett. **83**, 1010 (1999).
- [36] R. Ikeda, J. Phys. Soc. Jpn. **65**, 3998 (1996).
- [37] R. Ikeda, J. Phys. Soc. Jpn. **70**, No. 1 (2001).